

RSC Advances



This is an *Accepted Manuscript*, which has been through the Royal Society of Chemistry peer review process and has been accepted for publication.

Accepted Manuscripts are published online shortly after acceptance, before technical editing, formatting and proof reading. Using this free service, authors can make their results available to the community, in citable form, before we publish the edited article. This *Accepted Manuscript* will be replaced by the edited, formatted and paginated article as soon as this is available.

You can find more information about *Accepted Manuscripts* in the [Information for Authors](#).

Please note that technical editing may introduce minor changes to the text and/or graphics, which may alter content. The journal's standard [Terms & Conditions](#) and the [Ethical guidelines](#) still apply. In no event shall the Royal Society of Chemistry be held responsible for any errors or omissions in this *Accepted Manuscript* or any consequences arising from the use of any information it contains.

Microbial mediated synthesis, characterization, antibacterial and synergistic effect of gold nanoparticles using *Klebsiella pneumoniae* (MTCC- 4030)

P. Prema^a, A. Iniya^a and G. Immanuel^{b*}

^aResearch Department of Zoology, VHNSN College (Autonomous), Virudhunagar-626 001, Tamilnadu, India

^bCentre for Marine Science and Technology, Manonmaniam Sundaranar University Rajakkamangalam- 629502, Kanyakumari District, Tamilnadu, India

Abstract

In this research report the microbial mediated synthesis of gold nanoparticles (GNPs) was achieved by an easy biological protocol using *Klebsiella pneumoniae* (MTCC- 4030). Gold ions in the reaction mixture were exposed to *K. pneumoniae* for the formation of colloidal GNPs. The characterization study indicated that the UV-VIS spectral analysis of GNPs showed a peak at 550nm. The XRD spectroscopy of GNPs was confirmed by its crystalline nature. Scanning electron micrography of the GNPs showed spherical shape and was well dispersed. The atomic force microscopy revealed that the size range of GNPs was in between 10 and 15 nm. The FTIR study revealed that the possible involvement of reductive groups on the surface of nanoparticles. The antibacterial activity of GNPs showed highest inhibitory zone (25.60 mm) against *Escherichia coli* as indicator strain. The synergistic effect of GNPs gave highest fold increase (4.06) and activity index (3.210) against *E. coli*, followed by 2.610 activity index against *Staphylococcus aureus* using amoxycillin and streptomycin as standard antibiotics respectively.

* Corresponding author. Tel.: +91 4652 253078.

E-mail address: gimmas@gmail.com (G. Immanuel).

Introduction

Nanotechnology is one of the most blooming technologies of the current scenario. Role of microbial system for the synthesis of nanometals is rapidly gaining importance due to their optical, chemical, photo electrochemical and electronic properties. The thrust to develop reliable, ecofriendly procedures for the fabrication of nanoscale material is an important aspect of nanotechnology research. Gold nanoparticles (GNPs) have gained increasing interest due to their specific features such as unusual optical and electronic properties, non cytotoxicity, high

stability, biological compatibility, controllable morphology, size dispersion and easy surface functionalization.^{1,2} The green biosynthesis of nanoparticles can be achieved via the selection of an environmentally acceptable solvent with eco-friendly reducing and stabilizing agents.³ Biologically synthesized nanoparticles are naturally protein-capped, which prevents aggregation and avoids the use of external toxic capping agents. Srinath and Ravishankar Rai⁴ stated that this green biosynthesis is the method for the formation of monodispersed, small spherical GNPs of 4-10nm size by *K.pneumoniae* and it was the first report of attempting to improve the monodispersity and reduced size by varying gold salt concentration. Therefore; biological approaches on nanoparticle synthesis have been suggested as valuable alternatives to physical and chemical methods.⁵

Biological synthesis of nanoparticles has emerged as rapidly developing research area in nanotechnology across the globe with various biological entities being employed in production of nanoparticles constantly forming an impute alternative for conventional methods. Simple prokaryotes to complex eukaryotic organisms including higher plants are used for the fabrication of nanoparticels. Biosynthesis of GNPs has been reported in different prokaryotic organisms including *Bacillus subtili*⁶ *E.coli*,⁷ *Lactobacillus* sp.,⁸ *Pseudomonas aeruginosa*,⁹ *Rhodopseudomonas capsulate* etc.,¹⁰ however the molecular mechanisms involved in the metal ion reduction taking place for the synthesis of nanoparticles has not yet been established.

Nanoparticles can act as antibacterial and antifungal agents, due to their ability to interact with microorganisms. Exerting their antibacterial properties, nanoparticles attach to the surface of the cell. This interaction causes structural changes and damage, markedly disturbing vital cell functions, such as permeability, causing pits and gaps, depressing the activity of respiratory chain enzymes and finally leading to cell death.¹¹ The demonstrated antibacterial activity of nanoparticles recommends its possible application in the food preservation field; otherwise it can be applied as a potent sanitizing agent for disinfecting and sterilizing food industry equipment and containers against the attack and contamination with foodborne pathogenic bacteria.¹² In the present study, an attempt has been made on microbial mediated fabrication of GNPs by the reduction of H₂AuCl₄ ions using *K. pneumoniae* (MTCC- 4030). The fabricated GNPs were

characterized by UV, XRD, SEM, EDS, FTIR and AFM. Finally, the fabricated GNPs were applied in the field of antibacterial and synergistic studies in comparison with known antibiotics.

Results and Discussion

In the present study, the gram negative bacterium *K. pneumoniae* was found successful in synthesizing GNPs of uniform distribution and quite stable in the solution. The colour of the reaction solution turned from pale yellow to deep red indicated the formation of gold nanoparticles (Fig.1). The mechanism of extracellular biosynthesis of nanoparticles is proposed as a nitrate reductase-mediated synthesis that secretes the enzyme nitrate reductase, which then brings about bioreduction of metal ions and synthesis of nanoparticles.¹³ Both extracellular and intracellular methods are used for the synthesis of biological nanoparticles.¹⁴ The exact mechanism for the synthesis of nanoparticles using biological agents has not yet been elucidated, but it has been suggested that various biomolecules are responsible for the synthesis of nanoparticles. It seems that the cell wall of microorganisms play a major role in the intracellular synthesis of nanoparticles. Mukherjee *et al.*¹⁴ postulated that the mechanism of synthesis of nanoparticles occurs in three stages: trapping, bioreduction and synthesis. Honary *et al.*¹⁵ reported that the Enterobacteriaceae family's biomass to 1mM aqueous HAuCl₄ solution led to the development of a dark purple solution after 24h of reaction.

The UV-Visible spectroscopic result revealed that the reaction solution had an absorption maxima at 550nm attributed to the surface plasmon resonance band (SPR) of the gold nanoparticles (Fig.2). The optical absorption spectrum of metal nanoparticles was dominated by SPR, which shifted to longer wave lengths with increasing particle size. The reduction of HAuCl₄ to GNPs that can be identified from the peaks obtained around 650nm.¹⁶ Likewise, Skirtach *et al.*,¹⁷ reported that the absorption spectrum of GNPs was observed at 560nm, and it was synthesized using *P.aeruginosa*. It is well known that spherical nanoparticles of Au should exhibit single-surface plasmon bands, whereas anisotropic particles should exhibit two or three bands, corresponding to the quadrupole and higher multipole plasmon excitations.¹⁸

The FTIR spectrum of GNPs with absorption peaks of 1716, 1654, 1639, 1527, 1342, and 1249 cm⁻¹ are shown in Fig. 3. The strong peak at 1654 cm⁻¹ was identified as C=O due to carbonyl functional group. The peak at 1,527 cm⁻¹ showed the characteristic of N–O as an

asymmetric nitro compound. The small band at $1,639\text{ cm}^{-1}$ arised from the --C=C stretching vibrations corresponding to the --C=O due to carboxylic acid and carbonyl group. The small peak at 1249 cm^{-1} can be assigned to the C-N of aliphatic amine group. The presence of the intense peak at C=O stretching mode indicated the presence of carboxylic group in the material bound to GNPs. The lower wave numbers confirmed that the represented functional group combined with the GNPs and reduction occurred in that particular surface. Similarly, Sandt *et al*¹⁹ reported that the FTIR spectrum of another reference strain of *K. pneumoniae* displayed the wave number within the ranges of 763-775, 1053-1085 and 1555-1595 cm^{-1} . Honary *et al.*¹⁵ pointed out that the FTIR spectrum of the nanoparticles indicates the presence of various chemical groups, one of which is an amide. The presence of --COO-- , possibly due to amino acid residues may indicate that protein co-exists with the GNPs. An amide I band was observed at 1630 to 1650 cm^{-1} . This was further confirmed by the band at 3406 - 3412 cm^{-1} . The band at 1626 cm^{-1} corresponds to amide I due to carbonyl stretch in proteins.

XRD analysis is mainly taken to study the crystalline nature of the nanoparticles. The intensive diffraction peak at 2θ value of 38.20° from the (111) lattice plane of face centered cubic (fcc) gold unequivocally indicated that the particles were made of pure gold and was broad, while the (200) plane was less distinct ($2\theta = 44.4^\circ$). Two additional broad bands were observed at 64.60° (2θ) and 77.60° (2θ) and they correspond to the (220) and (311) planes of gold respectively (Fig. 4 and Table 1). In the obtained spectrum, the bragg's peak position and their intensities were compared with the standard JCPDS files (File No. JCPDS 4-0783). The obtained GNPs were found to be an average size of 26 nm with a cubic structure. The fraction between the intensity of the (200), (220) and (311) diffraction peaks was much lower, suggesting that the (111) plane is the predominant orientation.²⁰ Likewise, Prema and Thangapandiyani²¹ reported that the intensive diffraction peaks at 2θ value of 38.38° , 38.12° , 38° , and 38.24° corresponding to (111), (200), (220) lattice plane of face centered cubic (fcc) for unstabilized AuNPs and stabilized AuNPs respectively. Senapati²² reported that the GNPs produced by the *Fusarium oxysporum* had intense peaks at 38° (111), 45° (200), 67° (220) and 78° (311).

The morphology of the synthesized GNPs was observed under scanning electron microscopy (Fig.5). The micrograph of the scanning electron microscope indicated that the

synthesized particles were smaller sizes and almost spherical in shape and some of them were aggregated. Similarly, Biradar and Lingappa²³ revealed that the surface morphology of GNPs adhere to the surface in a scaly pattern. They have also observed that smaller sized particles were almost spherical in shape and some of them were aggregated.

The two and three dimensional images of GNPs were visualized by AFM (Figs. 6 and 7). The images revealed that the synthesized nanoparticles were in the form of spheres. GNPs were formed in several different sizes, ranging from small to large nanoparticles (10-40 nm). AFM data obtained in the present work revealed that the 3D profile showed strong shape control with a size around 10-15nm. Similarly, Srivastava *et al.*²⁴ reported that the 2D profile obtained by AFM suggested that the strong shape control with a size around 50nm. This strong shape control indicated that apart from reducing proteins present in the membrane bound fraction (MBF), certain organic groups must be acting as stabilizing agent.

The antibacterial activity of GNPs was investigated against the human bacterial pathogens such as *E.coli*, *S.epidermidis*, *S. aureus*, *P.aeruginosa*, and *B.subtilis* and the result on the inhibitory zone (mm) is represented in Table 2. GNPs gave the highest zone of inhibition (25.68mm) against *E. coli*, whereas the lowest zone of inhibition (18.70mm) was recorded against *S. aureus* as indicator strain. Similarly, an effective antimicrobial activity against *E.coli* and *S. aureus* using GNPs was reported earlier by Kim *et al.*²⁵

The result on synergistic effect of GNPs synthesized by *K. pneumoniae* is given in Table 3. It revealed that the distinct difference was observed between the inhibitory zones by antibiotics with and without GNPs. The enhanced zone of inhibition was observed and it was increased from 9 to 20 mm when the GNPs were incorporated with streptomycin antibiotics against *S. aureus*. Incontrast, the synergistic activity between GNPs and ampicillin, gentamycin, kanamycin, streptomycin and vancomycin was subsequently shown to be greater against *E.coli* and *P.aeruginosa* than against *S. aureus*. The highest fold increase (4.06) was observed against *P. aeruginosa*, followed by 3.52 fold increase was observed while using the combination of GNPs and streptomycin against *B. subtilis*. The two way ANOVA for the data on fold increase of GNPs against the selected bacterial pathogens revealed that the obtained data are statistically significant between antibiotics with GNPs and bacterial pathogens (F= 13.24 and 4.47; P < 0.05).

The zone of inhibition showed an increase in activity index for all the cases with a range between 1.10 and 2.25. The highest activity index (3.21) was observed against *E.coli* using amoxicillin as standard antibiotic, followed by 2.61 activity index was observed against *S. aureus* while compared with streptomycin (Table 4). The two way ANOVA for the data on activity index of GNPs against selected bacterial pathogens revealed that the obtained data are statistically significant between antibiotics with GNPs and bacterial pathogens ($F= 11.39$ and 3.45 ; $P < 0.05$). The present findings corroborate with the report of Shahverdi *et al.*²⁶, who stated that the increase in synergistic effects of penicillin G, amoxycillin, erythromycin, clindamycin and vancomycin in combination with the mycosynthesized GNPs against *E.coli*, *P. aeruginosa*, and *S. aureus*. Fayaz *et al.*²⁷ also reported the increase in antibacterial activity of ampicillin, kanamycin, erythromycin and chloramphenicol in combination with AuNPs against *S. typhi*, *E.coli*, *S. aureus* and *Micrococcus luteus*. Similarly, Agnihotri *et al.*²⁸ suggested that combined antibiotic therapy produce synergistic effects in the treatment of bacterial infection and has been shown to delay the emergence of antimicrobial resistance.

Conclusions

The overall results clearly emphasize the biobased approach towards the synthesis of GNPs has many advantages such as ease with which the process can be scaled up and economic viability. Applications of nanoparticles in medical and other fields make this method potentially use for the large-scale synthesis of other inorganic nanomaterials. Narrow size distribution and small nanosize GNPs also offer advantages for self-assembled monolayer formation and enhanced surface area. Gold colloidal solution is biologically well suited and has the potential to be used in medical and pharmaceutical applications due to their homologous size distribution.

Experimental Section

Chemicals and cultures

In the present study the chemicals used are Gold chloride (chloroauric acid; HAuCl_4), nutrient broth and nutrient agar, purchased from Himedia (P) Ltd., Mumbai, as starting materials without further purification. Sterile milliQ water was used throughout the experiment. Microorganism used in the experiment are *K. pneumoniae* (MTCC-4030), *E. coli* (MTCC-4296), *S. epidermidis*

(MTCC-435), *S. aureus* (MTCC-3160), *P. aeruginosa* (MTCC-424) and *B. cereus* (MTCC-619) were procured from the Microbial Type Culture Collection (MTCC), Chandigarh, India.

Fabrication of GNPs

A loopful culture of freshly grown *K. pneumoniae* was inoculated in 250ml conical flask containing 100 ml sterile nutrient broth. The inoculated medium was incubated at 37°C for 24 hrs in a rotary shaker at 120rpm. The overnight culture broth was centrifuged at 6000 rpm for 10 minutes and the supernatant was used for the synthesis of GNPs. To this cell-free supernatant, 1mM gold chloride was added, mixed well, and the solution was incubated at 37°C for 24 h.

Characterization of GNPs

Visual inspection. After 24 h of incubation, the preliminary detection of gold nanoparticles was done by visual observation of colour change in the culture filtrate.

UV–Visible spectroscopy analysis. The UV measurements was carried out on Shimadzu dual beam spectrophotometer (model UV – 1650 PC) operated at a resolution of 1nm using deionized water as the reference. The colloidal gold solution was transferred in to a quartz cuvette cell followed by immediate spectral measurements.

Fourier Transforms InfraRed Spectroscopy (FTIR) analysis. The synthesized colloidal gold solution was measured by Nicolet Impact 400FT-IR spectrophotometer using a spectral range of 4000 to 400 cm⁻¹ with a resolution of 4 cm⁻¹. Powder samples for the FTIR were prepared similarly as for powder diffraction measurements.¹⁵

X-Ray diffraction analysis. The crystallographic information about the colloidal gold solution was obtained from X-ray diffraction pattern. The XRD pattern was measured by a scanning mode of an X pert PRO PAN analytical instrument operated at 40KV and a current of 30mA with Cu K alpha radiations ($\lambda=1.5404 \text{ \AA}$) and the 2θ scanning range was of 30-80°C at 2° min⁻¹.

The average size of the particles was estimated by the following Debye Scherrer equation:

$$D = K\lambda/\beta \cos\theta$$

Where, D = thickness of the nano particles, K = constant, λ = wavelength of X-rays, β = width of half maxima of reflection, θ = Bragg angle

Scanning Electron Microscopy (SEM) study. The determination of nanoparticle morphology by high resolution analytical scanning electron microscopy (SEM) was performed using JEOL-6390 SEM instrument. Thin film of the sample was prepared on a carbon coated copper grid by just dropping the suspension of nanoparticles, extra solution was removed using blotting paper and then the film on the SEM grid was allowed to dry by putting it under a mercury lamp for 5 min. The sample surface images were taken at different magnifications.

Atomic Force Microscopy (AFM) study. AFM of GNPs was measured to know the exact particle size and the sample was characterized using Atomic Force Microscopy (Nanonics imaging MN1000) which measures the atomic range of particles using tapping mode.²⁹

Antibacterial activity of GNPs against human bacterial pathogens

Antibacterial assay. The antibacterial activity of synthesized GNPs was evaluated using agar well diffusion method proposed by Nithya *et al.*³⁰ Pure cultures of selected human pathogenic bacteria were subcultured individually in nutrient broth for 12hrs at 37°C. A 20ml volume of sterile Mueller Hinton Agar medium was poured into each petriplate and each bacterial strain was swabbed uniformly into plates using sterile cotton swabs. Wells of 6mm diameter were made onto each bacterium inoculated agar plate using sterile gel puncture. 100 μ l of GNPs suspension was introduced into the corresponding wells. The bactericidal activity was determined by a clear inhibition zone around the sample loaded well after incubation of plates overnight at 37°C.

Synergistic effect of GNPs. The synergistic effect of GNPs was carried out by disc diffusion method of Vadivel and Suja.³¹ To determine the synergistic effect, four standard antibiotic discs such as vancomycin, streptomycin, amikacin and amoxycillin were impregnated individually with 100 μ l each of freshly prepared GNPs and were placed onto the Mueller Hinton Agar medium inoculated with individual test organisms. Standard antibiotic discs alone were used as

positive controls. These plates were incubated overnight at 37°C. After incubation, the result was recorded by measuring the inhibitory zone diameter (mm).

Assessment of increase in fold area of zone of inhibition. The increase in fold area was assessed by the method of Birla *et al.*³² It was assessed by calculating the mean surface area of the inhibition zone generated by an antibiotic alone and in combination with GNPs by the following equation,

$$\text{Fold increase} = b^2 - a^2/a^2$$

Where a & b are the zone of inhibition for antibiotic alone and antibiotic with gold nanoparticles, respectively.

Activity Index. Activity Index of the synthesized GNPs was calculated according to the method of Singariya *et al.*³³ The inhibition zones were measured and compared with the standard reference antibiotics. The activity index for each sample was calculated by using the formula,

$$\text{Activity Index} = \frac{\text{Inhibition zone of the sample}}{\text{Inhibition zone of the standard}}$$

Statistical analysis

The data obtained in the present study were expressed as Mean \pm SD and was analysed using Two-way ANOVA at 5% level of significance using a computer software STATISTICA 06 (Statsoft, Bedford, UK).

Acknowledgements

The authors thank V.H.N.S.N. College Managing Board, Virudhunagar for providing facilities to complete the experiment in a successful manner.

Notes and references

- 1 M. Gericke and A. Pinches *Gold Bull.*, 2006, **39**, 22-28.
- 2 Md S. Nasir and H. Nur J. *Fund. Sci.*, 2008, **4**, 245-252.

- 3 P.Jegadeeswaran, R.Shivaraj and R.Venkatesh *Digest J. Nanomat. Biostruct.*, 2012, **7 (3)**, 991-998.
- 4 B.S.Srinath and V.Ravishankar Rai *3 Biotech.*,2015, **5**, 671-676.
- 5 P.Mohanpuria, N.K.Rana and S.K. Yadav *J. Nanopart. Res.*, 2008, **10 (3)**, 507-517.
- 6 T.J.Beveridge and R.G.E. Murray *J. Bacteriol.*, 1980, **141**,876-887.
- 7 S.Brown, M.Sarikaya and E. Johnson *J. Mol. Biol.*, 2000, **299**,725-735.
- 8 B.Nair and T. Pradeep *Cryst. Grow. Des.*, 2002, **2**, 293-298.
- 9 M.I.Husseiny, M. Abd El-Aziz, Y.Badr and M.A.Mahmoud *Spect. Acta A*, 2007, **67**,1003-1006.
- 10 S. He, Z.Guo, Y.Zhang, M.Zhang, J.Wang and N. Gu *Mat. Let.*, 2007, **61**,3984- 3987.
- 11 M.F. Zawrah and A.E. Sherein *Life Sci.J.*, 2011, **8(4)**, 37–44.
- 12 A.T.Ahmad, F.E.Weal and M.Shaadan *J. Food Safe*, 2010, **31**, 211-218.
- 13 S. A. Kumar, A.A.Ayoobul, A. Absar and M.I. Khan *J. Biomed. Nanotech.*,2007, **3**, 190–194.
- 14 P.Mukherjee, A.Ahmad, D.Mandal, S.Senapati, S.R.Sainkar, M.I.Khan, R.Ramani, R.Parischa, P.A.Kumar, M.Alam, M.Sastry and R. Kumar *Ange. Chem. Int. Ed.*, 2008, **40**, 3585–3588.
- 15 S. Honary, F.Eshrat Gharaei, Z.Khorshidi Paji and M.Eslamifar *Trop. J. Pharma Res.*, 2012, **11 (6)**, 887-891.
- 16 W.R.Li, X.B.Xie, Q.S.Shi, H.Y.Zeng, Y.S.Ou Yang and Y.B. Chen *Appl. Microbiol. Biotech.*, 2011, **85**, 1115- 1122.
- 17 A.G.Skirtach, C.Dejugnat, D.Braun, A.S.Susha, A.L.Rogach, W.J.Parak, H.Mohwald and G.B.Sukhorukov *Nano Lett.*, 2005, **5**,1371–1377.
- 18 W.Xu, Y.Wang, R.Xu, S.Liang, G.Zhang and D.Yin *J. Mat. Sci.*, 2007, **42**, 6942–6945.
- 19 C.Sandt, C.Madoulet, A.Kohler, P.Allouch, C. De Champs, M. Manfait and G.D. Sockalingam *J. Appl. Microbiol.*,2006, **101 (4)**, 785-797.
- 20 C.Malarkodi, S.Rajeshkumar, P.Vanaja, M.Kanniah Paulkumar, G.Gnanajobitha and G. Annadurai *J. Nanostruct. Chem.*, 2013, **3**,30-45.

- 21 P. Prema and S. Thangapandiyan *Int. J. Pharm. Pharmaceut. Sci.*, 2013, **5(1)**, 310-314.
- 22 S.Senapati, A.Ahmad, M.I.Khan, M.Sastry and R.Kumar *Small*, 2005, **1**, 517–520.
- 23 D. Biradar and K. Lingappa *World J. Sci. Tech.*, 2012, **2(2)**, 20-22.
- 24 S.K. Srivastava, R.Yamad, C. Ogino and A. Kondo *Nano Res. Lett.*, 2013, **8(1)**,70-78.
- 25 Y.J.Kim, S.H.Oh, H.J.Yi, Y.S.Kim, Y.Ko and S.J.Oh *J. Kor. Neurosur. Soc.*, 2007, **42(6)**, 441-446.
- 26 R.A. Shahverdi, S.Minaeian, R.H.Shahverdi, H.Jamalifar and A.A. Nohi *Process Biochem.*, 2007, **42**, 919-923.
- 27 A.M.Fayaz, K.Balaji, M.Giril, R. Yadav and P.T. Kalaichelvan *Nanomedicine. Nanotech. Biol. Med.*,2010, **6**, 103-106.
- 28 M.Agnihotri, S.Joshi, R.K.Ameeta, S.Zinjarde and S.Kulkarni *Materials Let.*, 2009, **63(15)**, 1231-1234.
- 29 A. Annamalai, S.Thomas Babu, N.Anna Jose, D.Sudha and V.L.Christina *World App. Sci. J.*, 2011, **13(8)**, 1833-1840.
- 30 G.Nithya, N.Hema Shepangam and M. Balaji *Arch. Appl. Sci. Res.*, 2011, **3**, 377-380.
- 31 S.Vadivel and S.Suja *J. Pharma Res.*, 2012, **5(2)**, 1268- 1272.
- 32 S.S. Birla, V.V.Tiwari, A.K.Gade, A.P.Ingle and M.K.Rai *Let. Appl. Microbiol.*, 2009, **48(2)**, 173-179.
- 33 P.Singariya, P.Kumar and K.K.Mourya *Int. J. Biol. Pharma Res.*, 2012, **3(2)**, 252-258.



Fig. 1 GNPs synthesized by *K. pneumoniae*

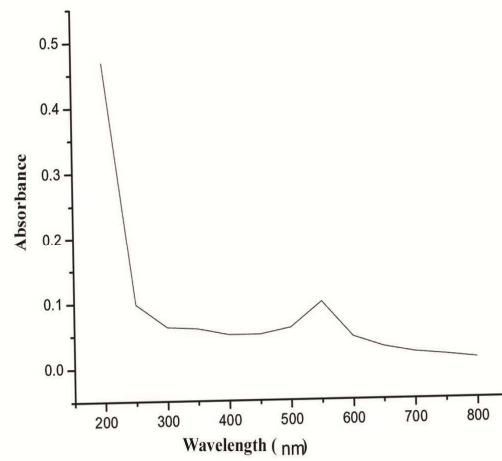


Fig. 2 UV-Vis Spectrum of GNPs synthesized by *K. pneumoniae*

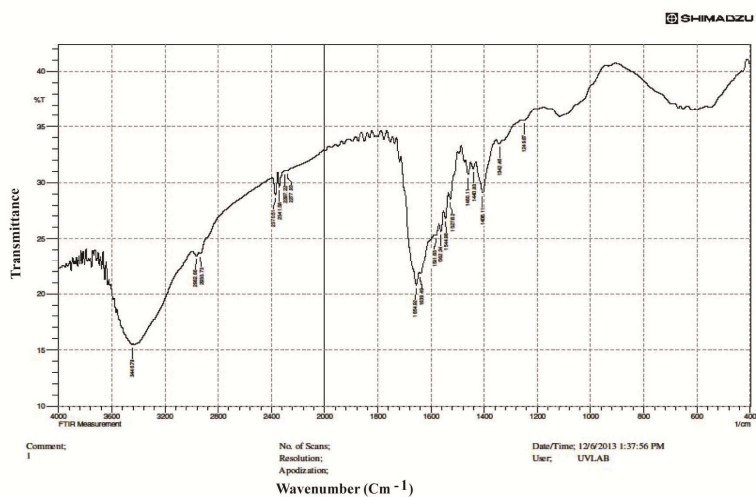


Fig. 3 FT-IR spectrum of GNPs synthesized by *K. pneumoniae*

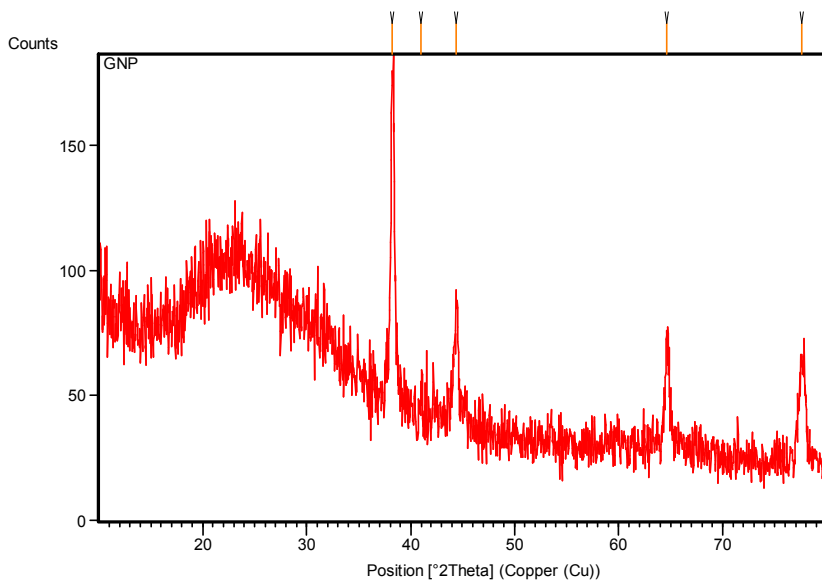


Fig. 4 X-Ray diffraction pattern of GNPs synthesized by *K. pneumoniae*

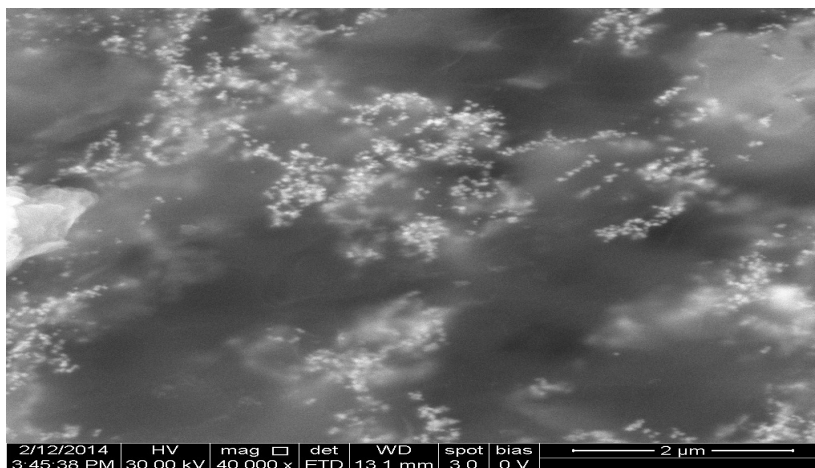


Fig. 5 Scanning electron micrograph of the synthesized GNPs

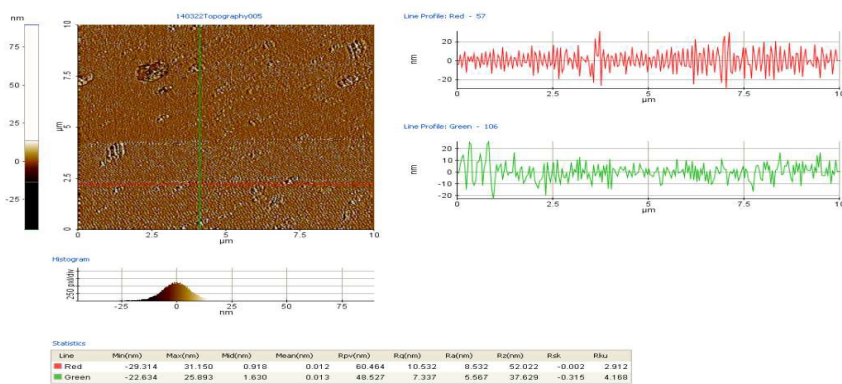


Fig. 6 AFM shows the two dimensional image of GNPs synthesized by *K. pneumoniae*

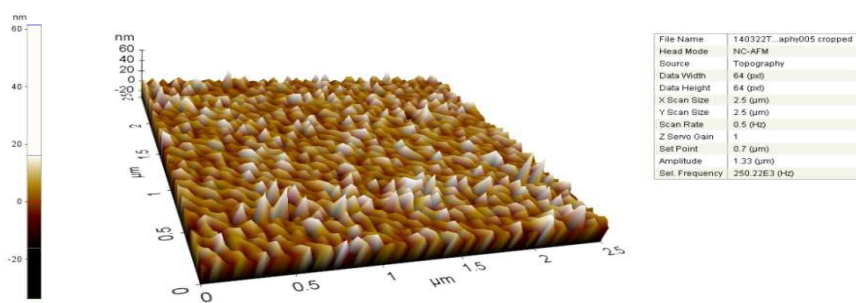


Fig. 7 AFM shows the three dimensional image of GNPs synthesized by *K. pneumoniae*

Table 1 X-ray diffraction peak list of GNPs synthesized by *K. pneumoniae*

Pos. [$^{\circ}$ 2Th.]	Height [cts]	FWHM Left [$^{\circ}$ 2Th.]	d-spacing [\AA]	Rel. Int. [%]
38.20(1)	83(24)	0.33(3)	2.35380	100.00
40.93(7)	9(9)	0.3(2)	2.20314	11.39
44.4(1)	34(30)	0.4(1)	2.03912	40.54
64.60(9)	38(34)	1(1)	1.44149	45.41
77.6(2)	24(80)	1(1)	1.22933	29.50

Table 2 Zone of Inhibition (mm) of GNPs synthesized by *K. pneumoniae* against selected bacterial pathogens

Bacterial Pathogens	Zone of Inhibition (Mean \pm SD)
<i>E. coli</i>	25.68 \pm 1.50
<i>S. epidermidis</i>	20.70 \pm 1.25
<i>S. aureus</i>	18.70 \pm 1.22
<i>P. aeruginosa</i>	20.90 \pm 0.92
<i>B. subtilis</i>	20.08 \pm 1.01

Each value is the Mean \pm SD of five individual replicates

Table 3 Synergistic effect of antibiotics in combination with or without GNPs against selected human bacterial pathogens

Pathogens	Antibiotics ($\mu\text{g}/\text{disc}$)	Zone of inhibition (mm)		Increased zone size (mm)
		Antibiotics alone	Antibiotics + GNPs	
<i>E.coli</i>	Amoxycillin (30 μg)	8.00 \pm 0.63	13.00 \pm 0.71	5.00 \pm 1.41 (1.640 \pm 0.013)*
	Amikacin (30 μg)	11.00 \pm 1.41	17.00 \pm 1.41	6.00 \pm 1.79 (1.390 \pm 0.007)
	Streptomycin (10 μg)	10.00 \pm 0.63	16.00 \pm 1.27	6.00 \pm 1.41 (1.560 \pm 0.012)
	Vancomycin (30 μg)	16.00 \pm 1.27	19.00 \pm 0.89	3.00 \pm 1.26 (0.410 \pm 0.010)
<i>S.epidermidis</i>	Amoxycillin (30 μg)	9.00 \pm 1.41	14.00 \pm 1.41	5.00 \pm 1.79 (1.420 \pm 0.007)
	Amikacin (30 μg)	12.00 \pm 1.26	16.00 \pm 1.27	4.00 \pm 1.41 (0.790 \pm 0.006)
	Streptomycin (10 μg)	10.00 \pm 0.63	16.00 \pm 1.41	6.00 \pm 1.79 (1.560 \pm 0.013)
	Vancomycin (30 μg)	18.00 \pm 1.60	22.00 \pm 1.79	4.00 \pm 1.41 (0.490 \pm 0.005)
<i>S.aureus</i>	Amoxycillin (30 μg)	9.00 \pm 1.41	18.00 \pm 1.60	9.00 \pm 0.63 (3.000 \pm 1.337)
	Amikacin (30 μg)	10.00 \pm 0.63	18.00 \pm 1.79	8.00 \pm 0.89 (2.240 \pm 0.008)
	Streptomycin (10 μg)	9.00 \pm 0.63	20.00 \pm 2.83	11.00 \pm 1.41 (3.040 \pm 0.009)
	Vancomycin (30 μg)	17.00 \pm 1.41	23.00 \pm 1.26	6.00 \pm 1.79 (0.830 \pm 0.004)
<i>P.aeruginosa</i>	Amoxycillin (30 μg)	8.00 \pm 0.63	18.00 \pm 1.79	10.00 \pm 0.63 (4.060 \pm 0.008)
	Amikacin (30 μg)	11.00 \pm 1.41	17.00 \pm 1.41	6.00 \pm 1.41 (1.390 \pm 0.007)
	Streptomycin (10 μg)	8.00 \pm 0.89	18.00 \pm 1.60	10.00 \pm 0.89 (4.060 \pm 0.005)
	Vancomycin (30 μg)	14.00 \pm 1.41	16.00 \pm 1.27	2.00 \pm 1.26 (0.310 \pm 0.007)
<i>B.cereus</i>	Amoxycillin (30 μg)	10.00 \pm 1.79	19.00 \pm 0.89	9.00 \pm 0.63 (2.610 \pm 0.014)
	Amikacin (30 μg)	12.00 \pm 1.26	19.00 \pm 0.63	7.00 \pm 0.89 (1.510 \pm 0.007)
	Streptomycin (10 μg)	8.00 \pm 0.89	17.00 \pm 1.41	9.00 \pm 1.41 (3.520 \pm 0.014)
	Vancomycin (30 μg)	14.00 \pm 1.41	20.00 \pm 2.83	6.00 \pm 1.79 (1.040 \pm 0.006)

Each value is the Mean \pm SD of five individual replicates.

*Values in paranthesis indicate fold increase of zone of inhibition

Table 4 Activity index of GNPs synthesized by *K.pneumoniae* against selected human bacterial pathogens in comparison with selected standard antibiotics

Antibiotics	Activity index /Pathogens				
	<i>E.coli</i>	<i>S.epidermidis</i>	<i>S.aureus</i>	<i>P.aeruginosa</i>	<i>B.cereus</i>
Amoxycillin (30 µg)	3.210 ± 0.010	2.300 ± 0.126	2.080 ± 0.009	2.610 ± 0.010	2.010 ± 0.013
Amikacin (30 µg)	2.330 ± 0.006	1.730 ± 0.006	1.870 ± 0.014	1.900 ± 0.048	1.670 ± 0.017
Streptomycin (10 µg)	2.570 ± 0.015	2.070 ± 0.015	2.080 ± 0.029	2.610 ± 0.006	2.510 ± 0.010
Vancomycin (30 µg)	1.610 ± 0.007	1.150 ± 0.006	1.100 ± 0.049	1.490 ± 0.007	1.430 ± 0.011

Each value is the Mean ± SD of five individual replicates